Aerosol and Air Quality Research

ORIGINAL RESEARCH
https://doi.org/10.4209/aaqr.210044

Simultaneous Measurements of $PM_{2.5}$- and PM_{10}-bound Benzo(a)pyrene in a Coastal Urban Atmosphere in Poland: Seasonality of Dry Deposition Fluxes and influence of Atmospheric Transport

Patrycja Siudek[1,2*], Wiesława Ruczyńska[2]

[1] Institute of Meteorology and Water Management – National Research Institute (IMWM-NRI), Waszyngtona 42, PL-81-342 Gdynia, Poland
[2] National Marine Fisheries Research Institute, Kołłataja 1, PL-81-332 Gdynia, Poland

ABSTRACT

Parallel 24-h measurements of $PM_{2.5}$- and PM_{10}-bound benzo(a)pyrene (BaP) were conducted in a coastal urban region in northern Poland in 2019. The aim was to examine distribution profiles, dry deposition fluxes and perform a trajectory analysis to investigate potential source regions of pollutants. The mean ratio of $PM_{2.5}/PM_{10}$ was 0.70 ± 0.23, suggesting significant heterogeneity in PM composition during the study period, both in fine and coarse fraction. The measurements revealed a strong seasonal variation in the concentration and dry deposition fluxes of BaP. The peak BaP concentrations of 6.14 ng m^{-3} and 6.65 ng m^{-3}, respectively in fine and coarse PM fractions were observed in December. They were directly attributed to local emission from major industrial (i.e., coal-fired power plants, refinery, solid waste burning, metal recycling plants) and residential sources (domestic heating units), and to the meteorological situation that led to the reduced dissipation of air pollutants and their transport outside the study domain. During the period from October to November, high Pb/Zn ratios in $PM_{2.5}$ and PM_{10} were also observed, suggesting significant contribution of industrial emission (coal combustion) and local non-exhaust traffic emissions, including tyre abrasion in the case of Zn and the resuspension of road dust rich in Pb. The highest daily BaP deposition fluxes of 2652 ng m^{-2} ($PM_{2.5}$) and 5561 ng m^{-2} (PM_{10}) were reported in winter, while the lowest values of daily BaP deposition (2 ng m^{-2}) were found during spring and summer measurements. Additionally, the three-dimensional FLEXTRA transport model was used to identify the impact of different sources on air masses over the study domain. FLEXTRA results showed that the air masses transported from distant S to W regions greatly affected the chemical composition of $PM_{2.5}$ and PM_{10} during autumn and winter.

Keywords: $PM_{2.5}$, PM_{10}, Urban-coastal region, Benzo(a)pyrene, Dry deposition fluxes

OPEN ACCESS

Received: March 2, 2021
Revised: July 9, 2021
Accepted: July 21, 2021

* **Corresponding Author:**
patrycja.siudek@gmail.com

Publisher:
Taiwan Association for Aerosol Research
ISSN: 1680-8584 print
ISSN: 2071-1409 online

1 INTRODUCTION

The role of atmosphere in the distribution and transformation of polycyclic aromatic hydrocarbons (PAHs) is crucial. Polycyclic aromatic hydrocarbons are emitted mainly from anthropogenic and industrial sources, including energy production, incomplete combustion of fossil fuels, coal and oil, iron/steel manufacturing, cement production, non-ferrous metal smelting, municipal waste incineration, vehicular emission (tyre/brake wear), petroleum refining, coke production and low-temperature processes such as wood burning (Slezakova *et al.*, 2007; Martiellini *et al.*, 2012; Pereira *et al.*, 2017; Ma *et al.*, 2018; Nguyen *et al.*, 2018; Yu *et al.*, 2018; Hsu *et al.*, 2019). The parent PAHs, such as naphthalene (*Nap*), acenaphthene (*Ace*), acenaphthylene (*Acy*), phenanthrene (*Phe*), fluorine (*Flu*), anthracene (*Ant*), benz(a)anthracene (*BaA*), chrysene (*Chry*), pyrene (*Pyr*),

fluoranthene (*Flt*), benzo(b)fluoranthene (*BbF*), benzo(k)fluoranthene (*BkF*), benzo(a)pyrene (*BaP*), dibenz(ah)anthracene (*DahA*), benzo(ghi)perylene (*BghiP*) and indeno(123-cd)pyrene (*IPy*), with molecular weight between 128 Da and 276 Da, have been identified by the U.S. Environmental Protection Agency as priority pollutants. These congeners are characterised by different molecular structure, volatility, photodegradation rate, reactivity, affinity to aerosol and organic ligands as well as reaction with gaseous pollutants. It has been previously demonstrated that PAHs may cause serious environmental problems, i.e., negative effects on plants, biota, air quality, water, soil system and public health (Eagar *et al.*, 2017). Therefore, the understanding of their seasonal variation is fundamental for further development of local and regional policy related to urban air quality and ecosystem protection.

PAHs are harmful pollutants that exhibit toxic properties. Benzo(a)pyrene is a key environmental indicator of air quality. It has toxic effects on the ecosystem and human health. A recent modelling study by Zhang and Tao (2009) has shown that the annual global emission of benzo(a)pyrene – the carcinogenic 5-benzene ring PAH, may reach 4.1×10^3 Mg, with predominant contribution from biofuel emission. Based on the results of 3-D GEOS-Chem model, Friedman *et al.* (2012) have found that the average particulate phase BaP concentrations can vary globally, with clear seasonal patterns for most of the considered locations. They provided empirical and modelling evidence for higher concentration levels of PAHs in the air and rainwater during winter in comparison with summer, highlighting highly influential role of factors such as transport, oxidation processes, gas-particle partitioning and variations in the emission (Friedman *et al.*, 2012). According to the European recommendation, the concentration of benzo(a)pyrene (BaP) in the inhalable air should not exceed 1 ng m^{-3}. However, the values of BaP registered in the urbanised areas of the European Union are often higher than the reference level (Ravindra *et al.*, 2008; Siudek and Frankowski, 2018).

PAHs are ubiquitous and they have important impact on the ecosystem. In polluted areas, PAHs are used for the estimation of the imprint of different anthropogenic sources related to incomplete coal combustion in the atmosphere. The coastal regions are regarded as hotspots of anthropogenic aerosols to the maritime atmosphere in the regional and global budgets (Roukos *et al.*, 2009). Several recent measurement campaigns have provided the evidence that coastal urban areas play a crucial role in determining the impact of gas- and particulate-phase PAHs on the air quality, climate system and public health (Khan *et al.*, 2016). In the coastal regions, the contribution of low- and high-molecular PAH congeners to the total PAH budget may vary largely between seasons, due to impact of different emission sources and meteorology (Staniszewska *et al.*, 2013; Siudek and Frankowski, 2018). Recent modelling work by Efstathiou *et al.* (2016) pointed out that ground-level concentrations of BaP within the southern Baltic Sea domain are higher than in other coastal areas (e.g., coasts of the Mediterranean Sea). Based on the existing data, Tsapakis *et al.* (2006) investigated PAHs cycling over the south-eastern Mediterranean Sea, showing their large spatial variability, shaped by long-range advection. They provided several interesting conclusions: (1) high concentrations of Flt and Pyr were registered in the gas phase, while elevated concentrations of BaP and Per were observed in the particulate phase, suggesting large contribution from coastal and ship emission plumes; (2) transfer of gaseous PAH congeners from the sea surface to the air was evident, and (3) almost 40% of the particulate PAHs over the Mediterranean environment was associated with smaller particles of < 0.5 μm, originating from shipping activities or photochemical transformations in air masses. The last observation is particularly interesting as it is typical to find different mass median diameters of PAHs in continental particles, i.e., in the accumulation (0.5–1.4 μm) and coarse modes of aerosol. The larger the particles are the shorter their residential time in the troposphere is. This fact may partly explain the significant reduction in PAHs emission in the Mediterranean Sea region.

In spite of the considerable progress in research studies within the Baltic Sea environment in recent years, the aerosol-related measurements are still less represented both in local and regional observations. Although the southern Baltic Sea is not well investigated in the context of atmospheric PAHs budgets, we can presume that these pollutants pose a threat to the environment of this area. Recent measurements of atmospheric PAH congeners in some other urbanised coastal regions have demonstrated that these compounds are mutagenic and toxic for marine biota and public health (Pekey *et al.*, 2007). The atmospheric processes of PAHs in the southern Baltic Sea are not well understood, mainly because this region is not adequately represented in

current environmental models and interdisciplinary field experiments. Therefore, taking into consideration the above facts, in this study, we performed daily simultaneous measurements of $PM_{2.5}$ and PM_{10}, at the coastal research platform, to examine the chemistry of a target and carcinogenic PAH – the BaP, with a special emphasis on its transformation and transport in the urban coastal atmosphere during four seasons. This first and in-depth case study of the seasonal cycle of BaP in fine and coarse particulate matter over the southern Baltic Sea has been undertaken in response to current and emerging scientific problems such as identification of major PAH sources associated with shipping activities and typical urban facilities, establish toxicity of $PM_{2.5}$-bound BaP and to determine conditions that influence BaP distribution and deposition within a study domain. Moreover, in this study we compare our results with those from other worldwide locations to consolidate recent knowledge on the atmospheric BaP chemistry and to better understand the relationships between toxic compounds, air quality and coastal environment.

2 MATERIALS AND METHODS

2.1 Details of the Experiment and Aerosol Collection

The 24-hour fine ($PM_{2.5}$) and coarse (PM_{10}) particulate matter samples for the comprehensive chemical analysis were collected from January/March to December 2019, at the coastal site in Gdynia (54°52'55.1''N, 18°56'13.5''E), Poland. Gdynia is a city in Pomorskie Province. Its area is 135.14 km^2 and it has up to 247 478 inhabitants. Gdynia can be characterised by high industrial, urban and traffic emissions. There is one of the biggest international harbours with shipbuilding industry (3,678 of incoming ships in 2016, BIP Gdynia). This city is a well-situated receptor area, suitable to investigate local and regional urban plumes, aerosol properties and long-range transport of pollutants originating from the surrounding countries, e.g., Germany, Belarus, Ukraine, Lithuania, Russia, Czech Republic, Slovakia and from Scandinavian countries. This region provides an excellent opportunity to examine the impact of shipping emission on aerosol chemistry, air quality and atmospheric processes. There are several dominant inland anthropogenic sources and shipping lanes within the study domain. The Google map of the sampling site is shown in Fig. 1, with major local emission sources such as coal-fired power plants, high traffic roads, domestic and commercial sectors, municipal solid waste recycling units, petrochemical plants and the refinery. In the vicinity of the sampling site there is also a large port area for various types of ships, i.e., small container ships, passenger vessels, cargo ships, etc.

In this study, the sampling instruments were mounted on the roof of Gdynia Aquarium. This building is located less than 100 metres from the shoreline. The sampling site was comprehensively equipped with a temperature-controlled set of automatic (PNS-18T Comde Derenda GmbH, Germany) and manual (LVS 3.1 Comde Derenda GmbH, Germany) samplers with a flow rate of 2.30 m^3 h^{-1}. The samplers contained meteorological sensors to register parameters such as air temperature, relative humidity, pressure, wind speed and direction. All the scientific instruments were installed on a special platform, about 4 m above flat-roof buildings, within the area clear of any obstacles, buildings and trees, in accordance with the European requirements for aerosol monitoring stations. After each daily measurement, environmental samples were immediately transported to the laboratory for subsequent analytical procedure. In this study, a total of 566 PM_{10} and $PM_{2.5}$ samples were obtained and examined for BaP distribution and seasonal variability. In addition, an impact of local/regional contaminant sources located within the study domain was assessed as well as biological risk related to atmospheric BaP over Gdynia. This experimental BaP-focused project was consistent with all criteria and requirements for basic research. The backward trajectory calculations were based on FLEXTRA air mass transport model. It was used to identify the impact of different sources on air masses over the study domain (Fig. 1), which we further discuss in the following sections.

During the entire sampling period, fine particulate matter concentrations ranged from 1.72 μg m^{-3} (July 29th) to 167 μg m^{-3} (February 17th), with the mean ± standard deviation of 24.1 ± 22.5 μg m^{-3}. Daily PM_{10} mass concentrations ranged from 3.45 μg m^{-3} to 65.5 μg m^{-3} (Table 1). However, it is important to highlight that PM_{10} was sampled from March to December. In both cases, higher values of mass PM concentrations were observed for the cold study period as compared to the warm period. This finding was mainly due to significant contribution of local

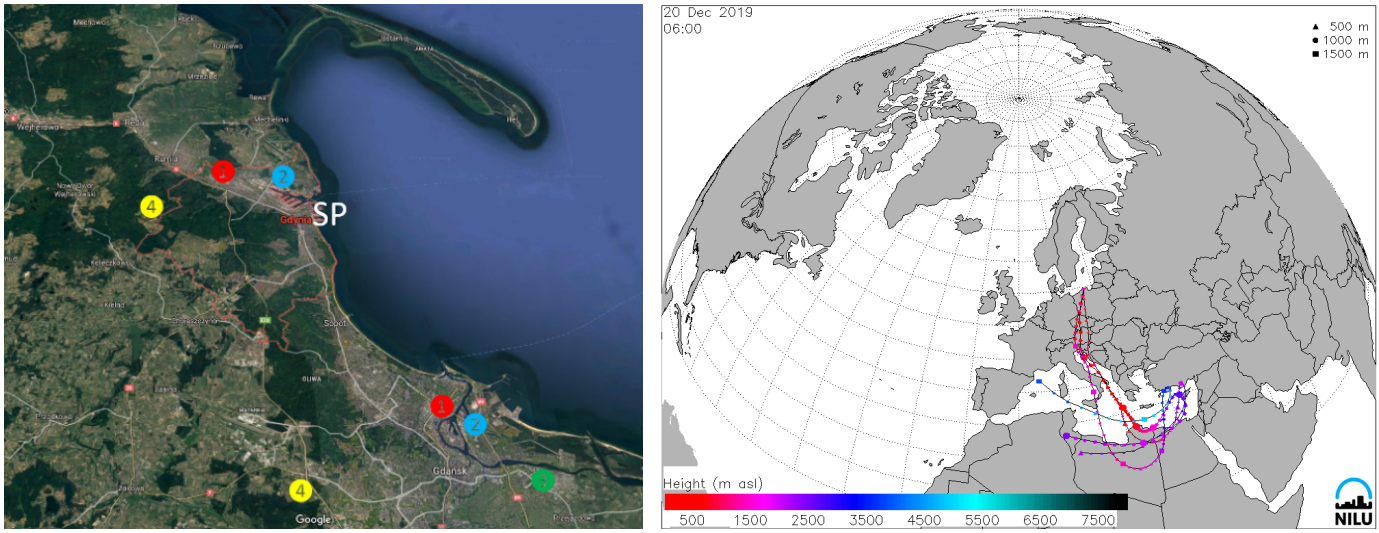

Fig. 1. Location of the sampling site (SP) in Gdynia, northern Poland, with colour circles representing major PAH sources: coal-fired power plants (red), port and docks area (blue), petrochemical refinery and plants (green), municipal solid waste recycling units (yellow) (left panel), and an example of one-day backward trajectory over the sampling site for a chosen day (with high BaP concentration and deposition fluxes) in the cold study period (results obtained from FLEXTRA model) (right panel).

Table 1. Descriptive statistics for $PM_{2.5}$ and PM_{10} mass concentrations and basic meteorological parameters in Gdynia, 2019. Note that $PM_{2.5}$ was sampled from January to December, while PM_{10} was sampled from March to December.

Meteorological parameter	Mean	SD	Median	Max	Min
Air temperature (°C)	9.54	6.75	8.65	25.20	–6.60
Air pressure (hPa)	1011	10.06	1011	1048	980
Relative humidity (%)	77.56	10.12	78.40	98.20	45.30
$PM_{2.5}$ (μg m^{-3})	24.26	22.52	18.97	1.72	167.24
PM_{10} (μg m^{-3})	19.05	10.31	17.24	65.52	3.45

high-temperature processes in residential (i.e., coal combustion, domestic heating units) and commercial sectors (coal-fired power plants) during the cold study period. The observations also confirmed that sampling days with high PM mass concentrations coincided with the specific meteorological situation (i.e., lower height of the mixing layer, lower temperature, higher relative humidity) and local chemistry-climate processes (NO_x, SO_2, CO).

Meteorological conditions over the study domain exhibited a large variation during the whole study period (Table 1). Specifically, the monthly mean air temperature ranged between –2.0°C (January) and 20.5°C (July). Regarding the ambient relative humidity (Rh), its mean value was 65%, the monthly peak was observed in January (mean of 75%) whereas the minimum in June (mean of 60%). The southerly winds blowing from industrial areas were much frequent during winter months, while for spring and summer observations strong westerly and southwesterly winds were predominant. An important meteorological feature of the study domain is that coastal winds from the north-to-east sectors are registered during spring and summer months. Moreover, the haze-fog episodes are typical of spring months.

2.2 Quantitative Analysis of Benzo(a)pyrene in $PM_{2.5}$ and PM_{10} Samples

The fine ($PM_{2.5}$) and coarse (PM_{10}) fractions of atmospheric particulate matter were collected on quartz microfiber filters (QMA, 47 mm in diameter, Whatman). In this study, the 3-step pre-treatment procedure was adopted to each filter before sampling, i.e., it was baked in a muffle furnace at 550°C for 8h, conditioned in a borosilicate glass desiccator under constant temperature and humidity (24°C and 40%) for 24 h, then weighted at the microbalance with 10 μg precision. Immediately after field sampling, the filters were packed in aluminum foil, conditioned for 24 h

in a glass desiccator, weighted and then folded again in aluminum foil and kept in a zipped bag at –20°C until the main analysis. All handling works with blanks, procedural and environmental filters were performed in a clean room equipped with HEPA units.

To determine the concentration of BaP in air samples, the quartz microfiber filters were extracted using Accelerated Solvent Extractor (ASE350 model, Dionex, UK). The accelerated extraction was applied under controlled pressure, temperature and time, which is recommended by U.S. EPA and described in method TO-13A. Such approach has been previously applied in many similar environmental studies (Li *et al.*, 2016). Here, dichloromethane and n-hexane in the ratio of 1:1 was used as a basic solvent. Briefly, 15 mL of DCM:*n*-hexane solvent (Merck) was added to the tightly-capped ASE cell containing one quarter of a filter. The extraction program was as follows: ASE350 system was heated to 100°C for 5 min, the pressure was maintained at 1500 psi and remained static for 15 min, then the system was cooled down to the lab temperature. Each filter was extracted 3 times in the same manner. After extraction, the raw aliquots were concentrated to about 1 mL in a rotatory evaporator at the bath temperature of 35°C. The sample extracts were then transferred to a pre-baked glass column filled with glass wood, 1 cm of anhydrous Na_2SO_4, 2 g of 2% activated silica gel and 1 cm of anhydrous Na_2SO_4 on top, and eluted with 20 mL of DCM and hexane mixture (1:1, v/v). Finally, the extracts were concentered via rotary evaporator in a vacuum to 1 mL and then gently evaporated to 0.5 mL under nitrogen stream in a 35°C water bath. After condensation, the extracts were transferred into glass chromatographic ampules and stored in a refrigerator until HPLC-FLD analysis.

Concentrations of benzo(a)pyrene in $PM_{2.5}$ and PM_{10} were quantitatively determined by Shimadzu modular Prominence HPLC system (Japan) coupled with fluorescence detection (excitation, λ = 290 nm, emission, λ = 430 nm). Data were proceeded through the use of Shimadzu Image v.5 software. The 5-ring PAH congener was quantified based on a several-point standard calibration curve (0.05; 0.02; 0.03; 0.05; 0.10; 0.15 μg mL^{-1}). The calibration curve was linear with a correlation coefficient (R^2) of 0.9999 for BaP. The PAHs standard solution in acetonitrile (100 μg BaP mL^{-1}, Chiron) was used to prepare sub-standards and determine the analysed congener in environmental air samples. The chromatographic separation of PAHs was obtained through the use of a Kinetex LC column (150 mm × 4.6 mm i.d., particle size of 3.5 μm, Phenomenex) and 50%:50% acetonitrile - deionized water as a mobile phase. The injection volume was 25 μL. The mobile phase flow was 0.5 mL min^{-1}. The method detection limit (MDL) for the measured BaP, expressed as three times the laboratory blanks, was on average 0.01 ng m^{-3}. In addition, the precision and accuracy of the analytical procedure were controlled using certified reference materials, i.e., ERM-CZ120 Fine dust. In general, 10 pre-cleaned QMA filters were loaded with 0.5 mg of CRM for PAHs quantification of recovery. The average recovery for the BaP analysis ranged between 88% and 105%. Field and procedural blanks were measured following the same procedure as in the case of environmental filters. The results from duplicate blanks represented less than 5% of the concentrations quantified in samples.

2.3 Calculation of BaP Dry Deposition Fluxes

The deposition fluxes of BaP ($\mathbf{F_{dry}}$) for each sampling day (ng m^{-2} day^{-1}) were calculated using the following equation:

$$F_{dry} = C_{BaP} \times V_d \quad (1)$$

where C_{BaP} is analyte concentration (ng m^{-3}) in the particulate phase of $PM_{2.5}$ or PM_{10}, and V_d is deposition velocity of particles during a sampling day (m s^{-1}). Here, it was assumed that V_d for fine particles was 0.5 cm s^{-1} (Rohde *et al.*, 1980; Poor *et al.*, 2004), while for coarse particles V_d was established at 1.0 cm s^{-1} (Zhang *et al.*, 2015). The monthly deposition fluxes of BaP were obtained by summing up the daily values, separately for $PM_{2.5}$ and PM_{10}.

2.4 Air Mass Trajectories

In order to investigate the sources of PAH congeners in $PM_{2.5}$ and PM_{10} over Gdynia, the air mass trajectory analysis was performed. The air mass transport models have been widely used in many aerosol-oriented studies (Forster *et al.*, 2001; Chang *et al.*, 2011; Halse *et al.*, 2011; Aalto

et al., 2015; Moroni *et al.*, 2015; ChooChuay *et al.*, 2020). In the present study, 24-h backward trajectories (BTs) were computed using a three-dimensional kinematic FLEXTRA air mass trajectory model (NILU and Institute of Meteorology and Geophysics, Vienna) with numerical meteorological data provided by European Centre for Medium Range Weather Forecast (ECMWF). This Lagrangian particle dispersion model has been described by Stohl *et al.* (1995). Specifically, the meteorological data used for each FLEXTRA trajectory simulation was analysed with a spatial resolution of 1.25 degree and temporal resolution of 6 hours. Three-dimensional trajectories were then calculated using the vertical wind provided by ECMWF. Stohl and Seibert (1998) have pointed out that accuracy of the trajectories is typically of the order of 20% of the travel distance, however uncertainties can also be much larger for individual cases. In the present study, the BTs were calculated for the period of 12th January–31th December, 2019 (6:00 UTC). In total, 340 BTs were calculated for the study domain, at three different arrival heights: 500, 1000 and 1500 m, to elucidate conditions below and over the boundary layer. In this study, nine separate air mass trajectory sectors were designated over the study domain. The sectors were marked as: **N** – north, **NE** – north-east, **E** – east, **SE** – south-east, **S** – south, **SW** – south-west, **W** – west, **NW** – north-west and **L** – local. Furthermore, the BTs and their contribution to the total number of air mass trajectories in each season were assigned to monthly deposition fluxes. The monthly mean deposition fluxes of $PM_{2.5}$- and PM_{10}-bound BaP were calculated for each season (spring, summer, autumn, winter) and discussed in Section 3.6.

3 RESULTS AND DISCUSSION

3.1 Monthly Distribution of the $PM_{2.5}$ to PM_{10} Ratio

As shown in Fig. 2, the mean mass ratios of $PM_{2.5}$/PM_{10} in Gdynia were significantly lower in June 2019 (0.35) than in the other months of the study period. It was found that the range of the $PM_{2.5}$/PM_{10} ratio was quite similar in August and September. The mean values of $PM_{2.5}$/PM_{10} observed in December and November were 0.78 and 0.92, respectively, and they were almost 1.4–1.6 times higher than the values reported in March.

It has been previously reported that lower $PM_{2.5}$ to PM_{10} ratio may indicate significant contribution of local sources of coarse airborne particles originating from road and construction

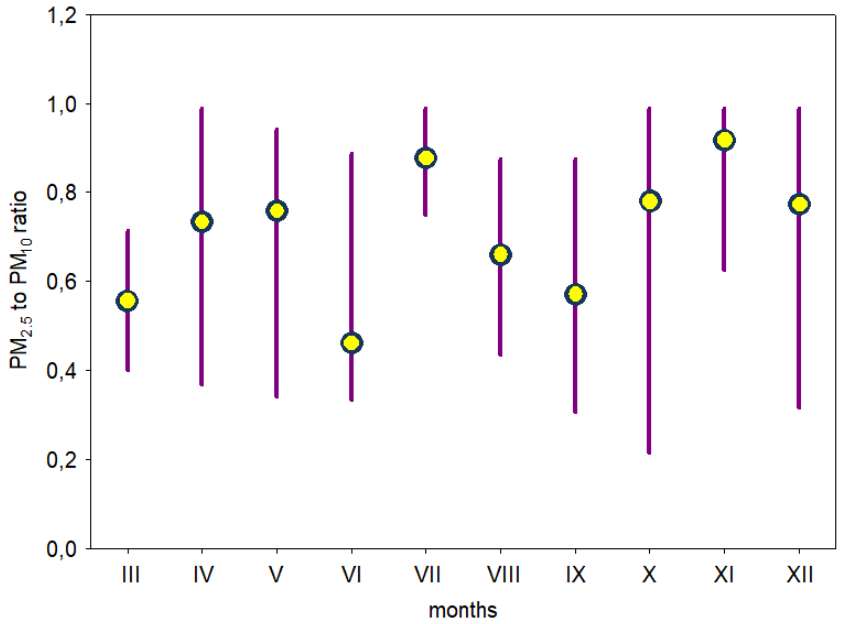

Fig. 2. Mean monthly variation in the mass ratio of $PM_{2.5}$ to PM_{10} registered during measurements in Gdynia, 2019. The lines indicate minimum and maximum values, while the circles correspond to the mean values of the $PM_{2.5}$/PM_{10} ratio. Results were obtained only for the period March–December, due to lack of PM_{10} data for January and February.

dust or sea salt aerosol and soil dust emissions (Slezakova *et al.*, 2007; Upadhyay *et al.*, 2011; Fang *et al.*, 2017; Siudek and Frankowski, 2018). On the other hand, the opposite trend may be mostly attributed to larger input of the primary $PM_{2.5}$ from vehicle emissions with a significant contribution from local coal burning, including power generation plants or residential heating (Xu *et al.*, 2017). For example, Permadi *et al.* (2018) have found that the observed values of the $PM_{2.5}/PM_{10}$ ratio ranged between 0.74 and 0.83 at the mixed urban sites in southeast Asia, suggesting predominant influence of road traffic, residential cooking and other urban activities. Ma and Jia (2016) have reported the annual mean $PM_{2.5}/PM_{10}$ ratios for three megacities in China, i.e., Beijing, Shanghai and Guangzhou, to be 0.63 ± 0.17, 0.69 ± 0.13 and 0.67 ± 0.06, respectively, indicating that the populations of fine and coarse particles were more heterogeneous, and pointing to the large variability in contribution of primary and secondary PM sources. Hsu *et al.* (2019) have found the mean $PM_{2.5}/PM_{10}$ ratio of 0.54 ± 0.35 at a single site in Taipei city, indicating that the role of fine particle fraction was predominant in shaping the urban air quality of that region. In the present study, the mean ratio of $PM_{2.5}/PM_{10}$ was 0.70 ± 0.23, suggesting significant heterogeneity in the PM composition both for fine and coarse fractions. The analysis of the $PM_{2.5}/PM_{10}$ ratio in Gdynia also revealed a seasonal trend of particulate matter and differences in emission sources during the study period. Similar findings have been demonstrated by Xu *et al.* (2017).

3.2 Seasonal Variation of the BaP Concentration in Gdynia

Table 2 shows temporal variations of BaP concentrations measured in $PM_{2.5}$ (from January to December) and PM_{10} (from March to December) in Gdynia. Seasonally, the BaP concentrations in $PM_{2.5}$ and PM_{10} were much higher during the cold study period (mean values of 1.59 ng m^{-3} and 1.857 ng m^{-3}, respectively) as compared to those registered in the warm study period (0.10 ng m^{-3} and 0.06 ng m^{-3}, respectively). The peak concentrations of BaP in fine (6.14 ng m^{-3}) and coarse (6.65 ng m^{-3}) PM fractions were observed in December 2019 (Table 2), i.e., in the period of heavy PAHs emission from local anthropogenic sources, i.e., coal-fired power plants, domestic heating units etc., and the specific meteorological situation which limited dissipation and transport of air pollutants outside the study domain. In this study, a simple statistical screening of possible relationships between selected variables was conducted. Correlations between BaP and meteorological parameters were different (Spearman coefficient, $p < 0.05$). In particular, BaP showed a higher negative correlation (–0.690) with temperature. This suggests that the ambient air temperature has significant impact on $PM_{2.5}$-bound BaP processes. A more detailed analysis for BaP/T correlations in different seasons revealed the following trend: autumn (–0.706) > winter (–0.564) > spring (–0.432) > summer (0.164). Previous studies in urban environments have mentioned that low temperature in a cold study period (autumn-winter) together with greater emission of particulate-phase PAHs from the residential/commercial heating sector and stagnant conditions can significantly enhance high concentration of 5-ring congeners in $PM_{2.5}$ and PM_{10}, while the increase in temperature during the summer period favours vaporization of

Table 2. Descriptive statistics for monthly benzo(a)pyrene concentrations (ng m^{-3}) in $PM_{2.5}$ and PM_{10} in Gdynia.

Month	$PM_{2.5}$			PM_{10}		
	mean ± 1 SD	min–max	median	mean ± 1 SD	min–max	median
January	1.56 ± 1.33	0.37–4.52	0.84			
February	1.13 ± 1.05	0.08–4.31	0.78			
March	0.62 ± 0.54	0.01–1.97	0.42	0.07 ± 0.03	0.04–0.09	0.07
April	0.33 ± 0.33	NA–1.19	0.20	0.23 ± 0.31	0.02–1.28	0.10
May	0.13 ± 0.15	NA–0.53	0.05	0.17 ± 0.21	0.02–0.89	0.08
June	0.03 ± 0.03	0.01–0.17	0.03	0.04 ± 0.03	NA–0.12	0.03
July	0.03 ± 0.04	NA–0.24	0.03	0.05 ± 0.07	0.01–0.38	0.03
August	0.08 ± 0.05	0.02–0.22	0.07	0.06 ± 0.04	NA–0.16	0.06
September	0.18 ± 0.17	0.01–0.64	0.12	0.03 ± 0.03	0.01–0.14	0.02
October	0.71 ± 0.58	0.03–2.94	0.59	0.46 ± 0.40	0.01–1.44	0.41
November	1.63 ± 1.29	0.28–5.90	**1.42**	1.70 ± 1.37	0.28–6.47	**1.38**
December	**1.74 ± 1.66**	0.06–**6.14**	1.06	**2.08 ± 2.10**	0.01–**6.65**	1.09

PAH from particle to gas phase and/or its rapid photochemical degradation (Wang *et al.*, 2016; Wang *et al.*, 2017).

In relation to air pressure, $PM_{2.5}$-bound BaP showed relatively low correlations (–0.116) during the whole sampling period. In contrast, the correlation for BaP versus relative humidity was weaker and positive (0.336). This result suggests that relative humidity can be identified as an important factor for BaP processes in the atmosphere over the Baltic coastal region. The similar dependencies have been reported by Wang *et al.* (2016).

Our results are in general agreement with some previous studies carried out in Poland (Staniszewska *et al.*, 2013; Wiśniewska *et al.*, 2019), western Europe (Amodio *et al.*, 2009; Pietrogrande *et al.*, 2011; Martellini *et al.*, 2012; Polachova *et al.*, 2020) and Asia (Chen *et al.*, 2016; Li *et al.*, 2016; Hsu *et al.*, 2019; Wang *et al.*, 2016; Wang *et al.*, 2017; Urbančok *et al.*, 2017; Gong *et al.*, 2018; Nguyen *et al.*, 2018). Additionally, relatively high BaP concentrations in both PM phases during winter study period can be explained by frequent occurrence of a thermal inversion layer (Hsu *et al.*, 2019) as well as low and/or below zero air temperature that directly favours rapid multiphase chemical reactions of organic compounds in the water phase of atmospheric particles, i.e., condensation and adsorption (Hsu *et al.*, 2019). Other factors that can explain elevated BaP concentrations in ambient air during winter are: low concentrations of ozone, reduced photochemical activity (Pietrogranade *et al.*, 2011) and high loadings of atmospheric particulate matter (Wang *et al.*, 2017).

As can be seen in Table 2, relatively low and less variable concentrations of BaP were registered between May and September for $PM_{2.5}$, and between March and September in the case of PM_{10}. This can be directly linked to significant changes in the local emission of PAHs and increasing role of atmospheric decomposition of 5-ring congeners (i.e., photo-, thermal- and heterogeneous chemical reactions with reactive gases). Several studies have highlighted the significant influence of high ambient temperature and strong oxidation capacity coupled with low relative humidity on the reduction processes of atmospheric BaP in summer (Hsu *et al.*, 2019). Furthermore, based on gas/particulate partitioning of PAHs in four seasons, Nguyen *et al.* (2018) have found that particulate 5-ring PAHs exhibited the lowest contribution in summer, whereas higher concentrations of particulate PAHs were observed in winter. Similar atmospheric transformations of PAHs could explain the observed BaP profiles in this study during the warm season.

3.3 Seasonal Variation of the BaP Deposition Fluxes in Gdynia

As shown in Fig. 3, high deposition fluxes of BaP in $PM_{2.5}$ and PM_{10} were predominant in winter. Specifically, the monthly mean $PM_{2.5}$-bound BaP deposition was as follows: 614 ng m^{-2} (Nov) > 459 ng m^{-2} (Dec) > 244 ng m^{-2} (Oct), suggesting the increase of BaP importance due to intensive PAHs emission from local combustion sources and the observed severe pollution events in December 2019. In comparison, during the cold study period, the median BaP deposition in PM_{10} ranged between 352 ng m^{-2} in October and 1100 ng m^{-2} in November (Fig. 3). The highest BaP deposition flux of 2652 ng m^{-2} day^{-1} in $PM_{2.5}$ was found on 16th December, while the lowest values (1 ng m^{-2} day^{-1}) were observed in April and May.

As for PM_{10}, the peak BaP deposition flux of 5561 ng m^{-2} day^{-1} was reported on 18th December, while the minimum BaP deposition (2 ng m^{-2} day^{-1}) was found in April and August. In Gdynia, the monthly mean BaP deposition fluxes in $PM_{2.5}$ substantially decreased from 365 ng m^{-2} in January to 85 ng m^{-2} in April, indicating a decrease in contribution of particulate PAHs during the period from spring to autumn (Fig. 3). In addition, the seasonal variability of BaP deposition fluxes at the coastal site in Gdynia was likely affected by meteorological conditions during the measurements (i.e., lower marine/planetary boundary layer height in winter vs. summer, stagnant conditions with low wind speed and high humidity that enhanced accumulation of air pollutants, seasonal differences in formation/decomposition processes in the coastal atmosphere, air temperature and relative humidity).

3.4 Comparison of the BaP Concentrations and Deposition Fluxes in Gdynia and Other Sites

The mean PM_{10}- and $PM_{2.5}$-bound benzo(a)pyrene concentrations measured in Gdynia in 2019 were 0.50 and 0.64 ng m^{-3}, respectively. These BaP levels were slightly lower than those observed

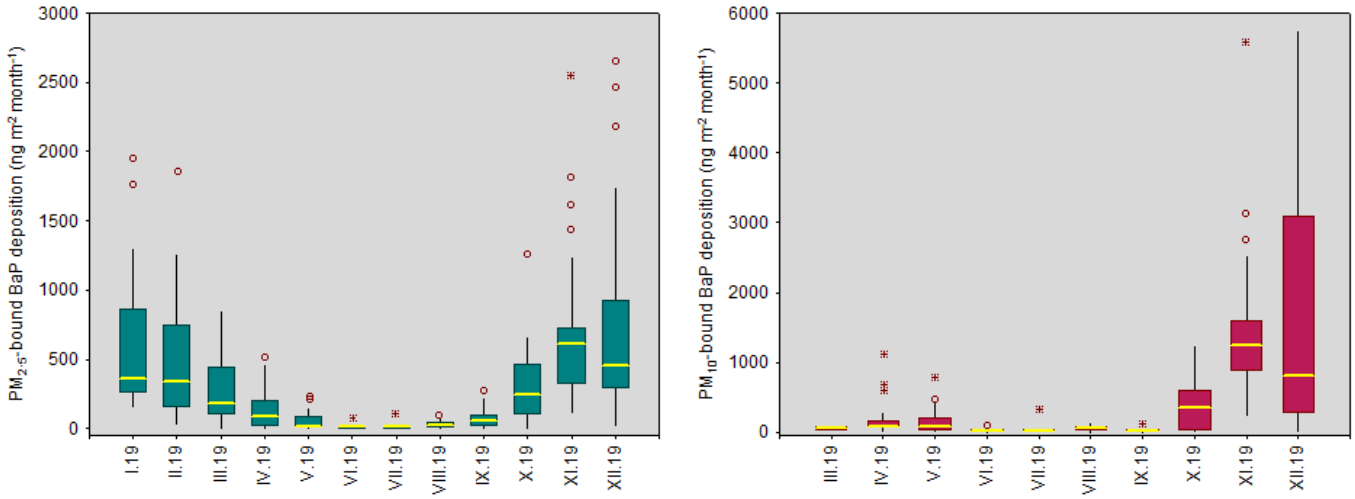

Fig. 4. Monthly variations in deposition fluxes of $PM_{2.5}$- (left plot) and PM_{10}-bound benzo(a)pyrene (right plot) at the coastal site in Gdynia, 2019. The lines inside boxes indicate mean values, whiskers - non-outlier range, circles - outliers, asterisks - extreme values and shaded boxes - 25th and 75th percentiles. Statistically significant differences ($p < 0.05$) in mean BaP concentrations were observed for the majority of months.

by Staniszewska *et al.* (2013) and Lewandowska *et al.* (2018), mostly due to lower frequency of severe pollution events during the heating season in 2019 as compared to previous PAHs-oriented measurements in 2008 and 2012.

A more detailed comparison of regional variations in BaP concentrations and deposition fluxes is presented in Table 3. A review study by Ma *et al.* (2018) have shown that atmospheric PAH concentrations across the Asian domain are the highest of all types of the considered measurement sites and that carcinogenic benzo(a)pyrene caused serious environmental problems. For example, the urban sites in Asia showed very variable concentrations of BaP in the ambient air, from < 1 ng m^{-3} measured in Hiroshima, Japan (Kakimoto *et al.*, 2002) to 16.6 ng m^{-3} in Kathmandu, Nepal (Chen *et al.*, 2015), with a mean value of 4.39 ng m^{-3} in Chengdu, China (Shi *et al.*, 2015), which was much higher than those obtained in suburban sites such as New Brunswick (Lee *et al.*, 2006). Moreover, Niu *et al.* (2017) showed extremely high mean values of BaP in $PM_{2.5}$ within Beijing-Tianjin-Hebei region (6.87–18.30 ng m^{-3}, Table 3). The mean BaP levels in other large urban/industrial regions of Asia, such as in Seoul (2.55 ng m^{-3}, Lee *et al.*, 2006), were much higher compared to Longyearbyen in Norway (0.89 ng m^{-3}, Drotikova *et al.*, 2020). It was also found that BaP concentrations in TPM at urban traffic/residential sites in Europe (Pietrogrande *et al.*, 2011; Martellini *et al.*, 2012; Siudek, 2018; Šišovic *et al.*, 2012), North America (Liu *et al.*, 2017) and Australia (Mishra *et al.*, 2016) were much lower than in similar urban areas of India (Ray *et al.*, 2017) and China (Shi *et al.*, 2015; Ma *et al.*, 2018). Such large spatial differences in the TPM-bound BaP concentrations are a combined effect, which can be linked to different sampling periods, impact of major local/regional PAH emission sources (increasing or decreasing trends, or absence of any trends), patterns in precipitation height, number of episodes with extremely high deposition fluxes of atmospheric PAH congeners.

As presented in Table 3, mean BaP concentrations in some rural locations of Asia, i.e., Ulsan, South Korea (0.16 ng m^{-3}, Nguyen *et al.*, 2018), Changhua, Taiwan (0.187 ng m^{-3}, Chen *et al.*, 2016), were lower than those at the coastal site in Gdynia. Season-depended features can significantly affect the annual and multi-year variability in BaP levels in a study region (Šišovic *et al.*, 2012; Ma *et al.*, 2018; Siudek, 2018). For example, Liu *et al.* (2017) have shown some significant temporal trends in atmospheric PAH concentrations and deposition values for a group of monitoring PAHs in the US. They have found that in the 1991–2005 period, the mean BaP concentration level in the urban ambient air was 0.35 ng m^{-3}. In addition, the areas in the U.K. included in a national program (1991–2005) showed annual mean BaP levels of 0.25 ng m^{-3} (Meijer *et al.*, 2008), while almost 10 times higher annual PM-bound BaP concentrations were identified in the mainland of China, including large cities such as Beijing, Chengdu, Dalian, Gangzhou, Nanchang, Shihezi,

Table 3. Mean benzo(a)pyrene concentrations (ng m^{-3}) and monthly deposition fluxes (ng m^{-2} $month^{-1}$) in Gdynia and other sites.

Site (country, domain)	Type	PM	BaP deposition	BaP concentration	Reference
Gdynia (Poland)	coastal	PM_{10}	404	0.50 (< MDL –6.65)	This study
Gdynia (Poland)	coastal	$PM_{2.5}$	294	0.64 (< MDL –6.14)	This study
Gdynia (Poland)	coastal			6.3/0.5 heating/non-heating	Lewandowska *et al.* (2018)
Gdynia (Poland)	coastal	TPM		2.18/0.05 heating/non-heating	Staniszewska *et al.* (2013)
Poznań (Poland)	urban	TPM		1.77	Siudek (2018)
Lochnagar (UK)	high-altitude		61		Arellano *et al.* (2018)
Pyrenees (Spain)	high-altitude		51		Arellano *et al.* (2018)
Tyrolean Alps (Austria)	high-altitude		20		Arellano *et al.* (2018)
Tatra Mountains (Slovakia)	high-altitude		280		Arellano *et al.* (2018)
Košetice (Czech Republic)	background site	TPM		0.4	Shahpoury *et al.* (2015)
Western Mediterranean Sea	coastal		183		Lipiatou *et al.* (1997)
Atlantic Ocean	coastal		25–75		Brun *et al.* (2004)
New Jersey	coastal		1.6		Gigliotti *et al.* (2005)
New Jersey	coastal		1.3–24		Gigliotti *et al.* (2005)
Tampa Bay	coastal		120		Poor *et al.* (2004)
Izmit Bay	Urban		1500		Pekey *et al.* (2007)
Manchester	Urban		9000		Halsall *et al.* (1997)
Cardiff	urban		6600		Halsall *et al.* (1997)
New Jersey	urban		42–54		Gigliotti *et al.* (2005)
Florence (Italy)	urban traffic	$PM_{2.5}$		0.049/0.47 summer/winter	Martellini *et al.* (2012)
Most city (Czech Republic)	urban	$PM_{2.5}$		0.002–3.2	Polachova *et al.* (2020)
Augsburg (Germany)	urban	$PM_{2.5}$		0.08/0.83 summer/winter	Pietrogrande *et al.* (2011)
Brisbane Metropolian Area (Australia)	traffic			0.02	Mishra *et al.* (2016)
Longyearbyen, Svalbard (Norway)	urban			0.89	Drotikova *et al.* (2020)
Győr (Hungary)	urban	PM_{10}		1.16	Szabo *et al.* (2015)
Kathmandu (Nepal)	urban	TPM		16.6	Chen *et al.* (2015)
Kolkata (India)	high-altitude	PM_{10}		5.3	Ray *et al.* (2017)
Darjeeling (India)	high-altitude			2.5	Ray *et al.* (2017)
Rio de Janeiro (Brazil)	urban	PM_{10}		0.268	Machado *et al.* (2009)
Chengdu (China)	urban			4.01	Shi *et al.* (2015)
Chengdu (China)	urban			4.39	Shi *et al.* (2015)
Changhua (Taiwan)	rural	$PM_{2.5}$		0.187	Chen *et al.* (2016)
Ulsan (South Korea)	semi-rural			0.16	Nguyen *et al.* (2018)
Hiroshima	suburban			0.3	Fon *et al.* (2007)
Tokyo	metropolitan city			0.63	Kakimoto *et al.* (2002)
Beijing (China)	urban	$PM_{2.5}$		7.92	Niu *et al.* (2017)
Tianjin (China)	urban	$PM_{2.5}$		6.87	Niu *et al.* (2017)
Shijiazhuang (China)	urban	$PM_{2.5}$		18.30	Niu *et al.* (2017)
Hengshui (China)	urban	$PM_{2.5}$		15.44	Niu *et al.* (2017)
Sapporo	urban			0.52	Kakimoto *et al.* (2002)
Kitakyushu	industrial			0.61	Kakimoto *et al.* (2002)
Seoul	urban			2.55	Lee *et al.* (2006)
Baltimore	urban			0.124	Lee *et al.* (2006)
Sao Paulo	urban			0.28	Lee *et al.* (2006)
New Brunswick	suburban			0.088	Lee *et al.* (2006)

Table 3. (*continued*).

Site (country, domain)	Type	PM	BaP deposition	BaP concentration	Reference
Zagreb	urban residential	PM_{10}		0.041/1.147 summer/winter	Šišovic *et al.* (2012)
Zagreb	urban traffic	PM_{10}		0.073/2.762 summer/winter	Šišovic *et al.* (2012)

Kumning, Lanzhou, Lhasa, Harbin, Xi'an (Ma *et al.*, 2018) and Korea (Park *et al.*, 2002). Recent long-term measurements at a European background site in Košetnice (Czech Republic) showed a large range for BaP concentrations in total particulate matter (< LOQ–9.1 ng m^{-3}, Shahpoury *et al.*, 2015), with a mean level of 0.4 ng m^{-3}, which was almost 4.5 times lower than in the city of Poznań, central Poland (Siudek, 2018).

The mean annual $PM_{2.5}$-BaP deposition flux in Gdynia amounted to 294 ng m^{-2}, which was much lower than that observed in Izmit Bay (1500 ng m^{-2} $month^{-1}$, Pekey *et al.*, 2007), Cardiff and Manchester (6600 and 9000 ng m^{-2} $month^{-1}$, respectively, Hallsal *et al.*, 1997). Arellano *et al.* (2018) have shown that BaP deposition fluxes at the European high-altitude stations such as Lochnagar (UK), Pyrenees (Spain) and Tyrolean Alps (Austria) are relatively low and vary between 20.0 and 61.0 ng m^{-2} $month^{-1}$, while in the Tatra Mountains the BaP deposition flux does not exceed 280 ng m^{-2} $month^{-1}$. In contrast, Gigliotti *et al.* (2005) have reported that BaP deposition values at some coastal sites in the North America tended to be one order of magnitude lower than the values from the Western Mediterranean Sea (Lipiatou *et al.*, 1997). The monthly BaP fluxes measured in the present study were relatively low compared to previous measurements by Lewandowska *et al.* (2018), largely due to some significant decrease in wintertime emission of PAHs from local sources in the sampling year of 2019.

According to the recent national inventory report (IIR, 2020), PAH emissions in Poland have shown a significant decreasing trend between 2010 (309.19 t) and 2018 (231.14 t). The largest national PAH source is fuel combustion in non-industrial combustion plants (mostly residential/commercial heating sector), contributing 81–82% to the total difference in the period of 2005–2018 (IIR, 2020). It should be noted that a large decline of 24% in the emission from residential sector have been reported for the period of 1990–2018, mainly due to replacing low-efficiency coal-fired boilers for more efficient devices and the implementation of thermomodernisation strategy (IIR, 2020). The second important anthropogenic origin of atmospheric PAHs is associated with industrial processes related to metal industry and other solvent and product usage as the dominant sub-sectors, followed by waste incineration and open burning of waste (IIR, 2020). The fugitive emission from fuels and field burning of agricultural residues are minor contributors to the national PAH emission.

In relation to the study region, it has been established that the BaP emission from residential/commercial sector (domestic heating, coal-fired power plants) amounted to 7 018.1 kg y^{-1}, which was 98.3% of the total anthropogenic emission at the provincial-scale in 2019 (Voivodeship raport, 2020). It is noteworthy that the BaP emission from industrial and transport sectors was 111.4 kg and 11.2 kg, respectively. The percentage of other sources was very low (< 0.01%, 0.27 kg y^{-1}).

3.5 Comparison of the Pb/Zn Ratios in $PM_{2.5}$ and PM_{10}

The geochemical data from observations in Poland related to the variability in metalliferous particles in inhalable fraction are still limited and more results are needed to consider the multi-year trends in atmospheric trace metal contents and their bioavailability (Siudek, 2021). In Gdynia, the monthly-averaged Pb/Zn ratios both in $PM_{2.5}$ and PM_{10} displayed a quite similar trend, indicating the consistency of their possible local/regional sources with industrial hotspots (Fig. 4).

For example, the highest monthly median Pb/Zn ratios of 0.37 and 0.35 for $PM_{2.5}$ and PM_{10}, respectively, were observed in December, while the lowest mean Pb/Zn ratios in the fine fraction were found in February (Fig. 4). It has to be noted that the Pb/Zn ratios in $PM_{2.5}$ revealed larger variability of concentration ranges as compared to PM_{10}, in particular for the period from September

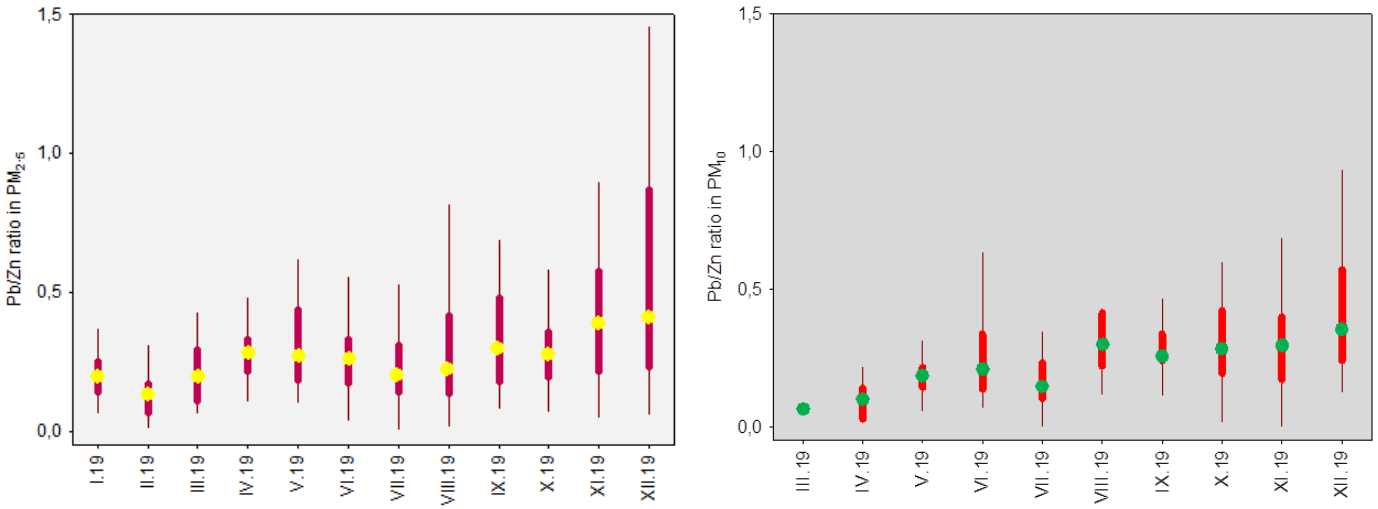

Fig. 4. The monthly variations in the Pb/Zn ratios in $PM_{2.5}$- (left) and PM_{10} (right) at the coastal site in Gdynia, 2019. The bars indicate 25th and 75th percentiles, thick vertical lines – maximum and minimum range, circles – median values. The statistically significant differences were observed ($p < 0.05$).

to December. This finding may suggest contribution from local non-exhaust traffic emissions, including tyre abrasion of Zn and resuspension of road dust rich in Pb. However, other anthropogenic sources (i.e., solid waste burning, metal recycling plants, industrial processes) are also possible. In Gdynia, the $PM_{2.5}$ and PM_{10}-bound Zn had different seasonal profile, suggesting the impact of local/regional sources related to natural soil resuspension and important role of industrial emission (coal-combustion). As presented in Fig. 1, the local Zn sources are associated with petrochemical refinery and plants, vehicular exhaust emission, and also with soil and road dust resuspension within the study domain and the surroundings. Amato *et al.* (2014) have found that urban roads are characterised by large content of crustal species such as Al, Ca, K, Ti, Fe and Mn with significant amount of Pb. They have also reported that the road dust emission reveals clear seasonality with maximum values in summer and minimum in winter (Amato *et al.*, 2014). Additionally, Garg *et al.* (2000) have reported that brake wear dust of motor vehicles contains large amount of Pb. In Gdynia, the local vehicle-related sources seemed to be more evident with winds (< 2 m s^{-1}) coming from the west and southwest.

Previous studies have highlighted that during winter measurements, local atmosphere can be more polluted and, consequently, the concentration of metallic elements such as Zn and Pb in PM samples can be significantly higher (Alastuey *et al.*, 2016), reflecting greater influence of local anthropogenic sources (i.e., coal combustion in power plants, shipping emission, waste incineration) and industrial activities (i.e., metallurgical processes). In Gdynia, we observed that this effect, similarly as in other polluted regions, was enhanced by thermal inversion layer and thick atmospheric mixing layer present in the cold study period, and this mitigated the transport of polluted particles up to higher altitudes leading to the significant impact of urban plumes on the study domain.

3.6 Seasonal Variation of the BaP Deposition in Relation to Air Mass Transport Sectors

It is well known that both local and regional emission of air pollutants combined with their atmospheric transport play a crucial role in depositional processes (Wang *et al.*, 2016). In this study, one of the priority issues was to examine the differences in dry deposition fluxes of BaP in relation to air mass trajectories. Table 4 shows that $PM_{2.5}$ and PM_{10}-bound BaP deposition fluxes over Gdynia vary seasonally depending on the air mass trajectory clusters, with maximum values reported in winter and minimum values in summer.

Specifically, in winter, the mean $PM_{2.5}$-bound BaP deposition fluxes associated with southern trajectories (SE–S–SW) were much higher than those attributed to local and northern trajectories (NW–N–NE). The daily mean deposition fluxes of $PM_{2.5}$-bound BaP from southern sectors during

Table 4. Mean $PM_{2.5}$ and PM_{10}-bound BaP deposition fluxes (ng m^{-2} day^{-1}) during measurements at the coastal site in Gdynia, 2019. Results were attributed to one of the nine clusters extracted from the FLEXTRA air mass trajectory model.

Season (months)	PM	AIR MASS TRAJECTORY SECTOR								
		N	NE	E	SE	S	SW	W	NW	L
Winter 19	$PM_{2.5}$	550.87	462.46	-	795.48	832.45	**986.05**	622.30	377.59	356.77
(I.19–II.19, XII.19)	PM_{10}	1582.69	650.36	-	-	2961.24	**3080.55**	1189.28	511.59	728.90
Spring 19	$PM_{2.5}$	272.76	76.60	130.11	134.69	226.95	**343.28**	123.23	112.81	223.15
(III.19–V.19)	PM_{10}	255.07	76.80	179.82	134.02	161.93	343.28	192.71	162.36	**590.66**
Summer 19	$PM_{2.5}$	14.14	12.17	5.33	16.39	21.74	34.02	23.89	17.38	**36.07**
(VI.19–VIII.19)	PM_{10}	33.41	34.52	14.26	32.63	28.08	47.72	47.37	54.37	**54.95**
Autumn 19	$PM_{2.5}$	264.73	42.48	224.94	**528.35**	472.47	495.34	247.92	145.52	93.77
(IX.19–XI.19)	PM_{10}	504.92	18.38	53.41	363.35	**1229.96**	985.37	267.19	124.68	21.40
ALL	$PM_{2.5}$	227.39	119.28	125.84	266.65	454.75	**478.30**	266.68	161.32	136.41
	PM_{10}	372.56	88.74	121.42	155.14	**1029.02**	924.95	370.86	134.87	222.78

the winter measurements decreased as follows: 986.05 ng m^{-2} day^{-1} (SW) > 832.45 ng m^{-2} day^{-1} (S) > 795.48 ng m^{-2} day^{-1} (SE). The PM_{10}-bound BaP deposition fluxes also revealed a similar pattern during the winter study period, i.e., higher values were found for SW (3080.55 ng m^{-2} day^{-1}) and S (2961.24 ng m^{-2} day^{-1}) sectors, while lower values were determined for the other sectors (Table 4). As reported by Lewandowska *et al.* (2018), when winter air masses originated from distant southern areas of Poland and Europe, they could transport higher loads of PAH-rich particles and therefore the deposition fluxes of air pollutants in Gdynia could be higher. Furthermore, most recent PAHs-oriented studies by Siudek (2018) have demonstrated a significant contribution of particulate-phase pollutants originating from industrial/urban and non-local sources in central Poland during autumn and winter study periods. However, it should be highlighted that the domestic heating from local residential sector had a predominant role in the total budget of PM. Previous studies have reported that the emissions from coal and wood burning in domestic systems of urban areas are much higher in winter than in a warm study period due to higher supply for energy. Here, daily mean $PM_{2.5}$-bound deposition fluxes in spring were highest for the SW sector (343.28 ng m^{-2}) followed by N (272.76 ng m^{-2}), S (226.95 ng m^{-2}) and local clusters (223.15 ng m^{-2}), while the lowest deposition fluxes were observed for the NE cluster (76.60 ng m^{-2}, Table 4). In contrast, daily mean PM_{10}-bound BaP deposition fluxes of 590.66 ng m^{-2} were found for the local cluster. This was at least 2 times higher as compared to the other clusters (range: 76.80–255.07 ng m^{-2}), indicating that there were significant differences in the deposition of BaP during spring measurements.

The results of $PM_{2.5}$-bound and PM_{10}-bound BaP showed that the summer deposition fluxes were below 60 ng m^{-2} day^{-1} for all clusters, and the highest values were associated with the local cluster (local traffic emission, shipping emission). In comparison with summer measurements, the values of BaP deposition fluxes in autumn months were much higher for both size-mode particles. Specifically, the highest mean daily PM_{10}-bound BaP deposition flux of 1229.96 ng m^{-2} was measured for the S cluster, while the highest deposition of BaP in $PM_{2.5}$ (528.35 ng m^{-2}) was found for the SE cluster. As mentioned in some previous studies, due to higher air temperatures in summer, the condensation of most volatile PAHs can be significantly reduced and, as a consequence, the deposition fluxes are typically lower compared to other seasons (Arellano *et al.*, 2018). Some similar trend was observed in this study.

4 CONCLUSIONS

Simultaneous measurements of $PM_{2.5}$ and PM_{10} samples in a coastal urban region of northern Poland were performed for the first time in 2019 to determine the seasonality of $PM_{2.5}$ and PM_{10}-bound benzo(a)pyrene, the target congener of five-ring PAHs. The concentrations of BaP were quantitatively determined by HPLC-FLD. The seasonal variability of BaP concentrations and deposition fluxes was evident. The highest values were observed in winter, being the result of large emission from local residential sector (domestic heating units) and major industrial sources (i.e., coal-fired power plants, refinery, solid waste burning, metal recycling plants) as well as

meteorological situation leading to the reduced dissipation of air pollutants and their limited transport outside the study domain. In contrast, summer measurements exhibited considerably lower BaP concentrations and deposition fluxes in particulate matter over this coastal urban region, which was likely related to a decrease in local coal combustion (commercial and residential), vaporization of PAHs from particle to gas phase and/or its rapid photochemical degradation. It was also observed that the local traffic emission played a significant role. The large-scale atmospheric transport of air pollutants from distant industrially-impacted regions may influence the coastal aerosol population in the southern Baltic Sea, especially in winter.

The limitation of this study is that we have not addressed the influence of precipitation amount on the deposition fluxes of BaP during the sampling period, as considered by Staniszewska *et al.* (2013). Due to lack of routine PM_{10} measurements in January and February 2019, the obtained values of the dry deposition flux in coarse fraction for winter 2019, in all selected sectors, can be underestimated.

ACKNOWLEDGMENTS

This research was financially supported by National Science Center in Poland (UMO-2017/27/B/ST10/01200). In this paper, the modeling results from FLEXTRA were used and thus special thanks go to ECMWF, NILU and the model developers. Authors appreciate K. Wiśniewska's and A. Lewandowska's help with PM sampling. Thanks also go to I. Waszak for taking part in the purification of extracts.

REFERENCES

Aalto, T., Hatakka, J., Kouznetsov, R., Stanislawska, K. (2015). Background and anthropogenic influences on atmospheric CO_2 concentrations measured at Pallas: Comparison of two models for tracing air mass history. Boreal Environ. Res. 20, 213–226.

Alastuey, A., Querol, X., Aas, W., Lucarelli, F., Pérez, N., Moreno, T., Cavalli, F., Areskoug, H., Balan, V., Catrambone, M., Ceburnis, D., Cerro, J.C., Conil, S., Gevorgyan, L., Hueglin, C., Imre, K., Jaffrezo, J.L., Leeson, S.R., Mihalopoulos, N., Mitosinkova, M., *et al.* (2016). Geochemistry of PM_{10} over Europe during the EMEP intensive measurement periods in summer 2012 and winter 2013. Atmos. Chem. Phys. 16, 6107–6129. https://doi.org/10.5194/acp-16-6107-2016

Amato, F., Alastuey, A., de la Rosa, J., Gonzalez Castanedo, Y., Sánchez de la Campa, A.M., Pandolfi, M., Lozano, A., Contreras González, J., Querol, X. (2020). Trends of road dust emissions contributions on ambient air particulate levels at rural, urban and industrial sites in southern Spain. Atmos. Chem. Phys. 14, 3533–3544. https://doi.org/10.5194/acp-14-3533-2014

Amodio, M., Caselli, M., de Gennaro, G., Tutino, M. (2009). Particulate PAHs in two urban areas of southern Italy: Impact of the sources, meteorological and background conditions on air quality. Environ. Res. 109, 812–820. https://doi.org/10.1016/j.envres.2009.07.011

Arellano, L., Fernandex, P., van Drooge, B.L., Rose, N.L., Nickus, U., Thies, H., Stuchlik, E., Camarero, L., Catalan, J., Grimalt, J.O. (2018). Drivers of atmospheric deposition of polycyclic aromatic hydrocarbons at European high-altitude sites. Atmos. Chem. Phys. 18, 16081–16097. https://doi.org/10.5194/acp-18-16081-2018

Brun, G.L., Vaidya, O.C., Léger, M.G. (2004). Atmospheric deposition of polycyclic aromatic hydrocarbons to Atlantic Canada: Geographic and temporal distributions and trends 1980-2001. Environ. Sci. Technol. 38, 1941–1948. https://doi.org/10.1021/es034645l

Chang, R.Y.W., Leck, C., Graus, M., Müller, M., Paatero, J., Burkhart, J.F., Stohl, A., Orr, L.H., Hayden, K., Li, S.M., Hansel, A., Tjernström, M., Leaitch, W.R., Abbatt, J.P.D. (2011). Aerosol composition and sources in the central Arctic Ocean during ASCOS. Atmos. Chem. Phys. 11, 10619–10636. https://doi.org/10.5194/acp-11-10619-2011

Chen, P., Kang, S., Li, C., Rupakheti, M., Yan, F., Li, Q., Ji, Z., Zhang, Q., Luo, W., Sillanpää, M. (2015). Characteristics and sources of polycyclic aromatic hydrocarbons in atmospheric aerosols in the Kathmandu Valley, Nepal. Sci. Total Environ. 538, 86–92. https://doi.org/10.1016/j.scitotenv.2015.08.006

Chen, Y.C., Chaing, H.C., Hsu, C.Y., Yang, T.T., Lin, T.T., Chen, M.J., Chen, N.T., Wu, Y.S. (2016). Ambient $PM_{2.5}$-bound polycyclic aromatic hydrocarbons (PAHs) in Changhua country, central Taiwan: Seasonal variation, source apportionment and cancer risk assessment. Environ. Pollut. 218, 372–382. https://doi.org/10.1016/j.envpol.2016.07.016

ChooChuay, C., Pongpiachan, S., Tipmanee, D., Deelaman, W., Suttinun, O., Wang, Q., Xing, L., Li, G., Han, Y., Palakun, J., Poshyachinda, S., Aukkaravittayapun, S., Surapipith, V., Cao, J. (2020). Long-range transboundary atmospheric transport of polycyclic aromatic hydrocarbons, carbonaceous compositions, and water-soluble ionic species in southern Thailand. Aerosol Air Qual. Res. 20, 1591–1606. https://doi.org/10.4209/aaqr.2020.03.0120

Drotikova, T., Ali, A.M., Halse, A.K., Reinardy, H.C., Kallenborn, R. (2020). Polycyclic aromatic hydrocarbons (PAHs) and oxy- and nitro-PAHs in ambient air of the Arctic town Longyearbyen, Svalbard. Atmos. Chem. Phys. Discuss 20, 9997–10014. https://doi.org/10.5194/acp-20-9997-2020

Eagar, J.D., Ervens, B., Herckes, P. (2017). Impact of partitioning and oxidative processing of PAH in fogs and clouds on atmospheric lifetimes of PAH. Atmos. Environ. 160, 132–141. https://doi.org/10.1016/j.atmosenv.2017.04.016

Efstathiou, C.I., Matejovičová, J., Bieser, J., Lammel, G. (2016). Evaluation of gas-particle partitioning in a regional air quality model for organic pollutants. Atmos. Chem. Phys. 16, 15327–15345. https://doi.org/10.5194/acp-16-15327-2016

Fang, G.C., Xiao, Y.J., Zhuang, Y.J., Cho, M.H., Huang, C.Y., Tsai, K.H. (2017). $PM_{2.5}$ particulates and metallic elements (Ni, Cu, Zn, Cd and Pb) study in a mixed area of summer season in Shalu, Taiwan. Environ. Geochem. Health 39, 791–802. https://doi.org/10.1007/s10653-016-9848-7

Fon, T.Y.W., Noriatsu, O., Hiroshi, S. (2007). Polycyclic aromatic hydrocarbons (PAHs) in the aerosol of Higashi Hiroshima, Japan: Pollution scenario and source identification. Water Air Soil Pollut. 182, 235–243. https://doi.org/10.1007/s11270-007-9335-y

Forster, C., Wandinger, U., Wotawa, G., James, P., Mattis, I., Althausen, D., Simmonds, P., O'Doherty, S., Jennings, S.G., Kleefeld, C., Schneider, J., Trickl, T., Kreipl, S., Jager, H., Stohl, A. (2001). Transport of boreal forest fire emissions from Canada to Europe. J. Geophys. Res. 106, 22887–22906. https://doi.org/10.1029/2001JD900115

Friedman, C.L., Selin, N.E. (2012). Long-range atmospheric transport of polycyclic aromatic hydrocarbons: A global 3-D model analysis including evaluation of arctic sources. Environ. Sci. Technol. 46, 9501–9510. https://doi.org/10.1021/es301904d

Garg, B.D., Cadle, S.H., Mulawa, P.A., Groblicki, P.J., Laroo, C., Parr, G.A. (2000). Brake wear particulate matter emissions. Environ. Sci. Technol. 34, 4463–4469. https://doi.org/10.1021/es001108h

Gigliotti, C.L., Totten, L.A., Offenberg, J.H., Dachs, J., Reinfelder, J.R., Nelson, E.D., Glenn, T.R., Eisenreich, S.J. (2005). Atmospheric concentrations and deposition of polycyclic aromatic hydrocarbons to the Mid-Atlantic East Coast Region. Environ. Sci. Technol. 39, 5550–5559. https://doi.org/10.1021/es050401k

Gong, P., Wang, X., Sheng, J., Wang, H., Yuan, X., He, Y., Qian, Y., Yao, T. (2018). Seasonal variations and sources of atmospheric polycyclic aromatic hydrocarbons and organochlorine compounds in a high-altitude city: Evidence from four-year observations. Environ. Pollut. 233, 1188–1197. https://doi.org/10.1016/j.envpol.2017.10.064

Halsall, C.J., Coleman, P.J., Jones, K.C. (1997). Atmospheric deposition of polychlorinated dibenzo-p-dioxins/dibenzofurans (PCDD/Fs) and polycyclic aromatic hydrocarbons (PAHs) in two UK cities. Chemosphere 35, 1919–1931. https://doi.org/10.1016/S0045-6535(97)00265-8

Halse, A.K., Schlabach, M., Eckhardt, S., Sweetman, A., Jones, K.C., Breivik K. (2011). Spatial variability of POPs in European background air. Atmos. Chem. Phys. 11, 1549–1564. https://doi.org/10.5194/acp-11-1549-2011

Hsu, C.Y., Chiang, H.C., Chen, M.J., Yang, T.T., Wu, Y.S., Chen, Y.C. (2019). Impacts of harazdous metals and PAHs in fine and coarse particles with long-range transport in Taipei city. Environ. Pollut. 250, 934–943. https://doi.org/10.1016/j.envpol.2019.04.038

Informative Inventory Report (IIR) (2020). Submission under the UN ECE Convention on Long-range Transboundary Air Pollution and Directive (EU) 2016/2284 Air pollutant emissions in Poland 1990–2018, Warszawa, 1–254.

Kakimoto, H., Matsumoto, Y., Sakai, S., Kanoh, F., Arashidani, K., Tang, N., Akutsu, K., Nakajima,

A., Awata, Y., Toriba, A., Kizu, R., Hayakawa, K. (2002). Comparison of atmospheric polycyclic aromatic hydrocarbons and nitro polycyclic aromatic hydrocarbons in an industrialized city (Kitakyushu) and two commercial cities (Sapporo and Tokyo). J. Health Sci. 48, 370–375. https://doi.org/10.1248/jhs.48.370

Khan, M.B., Masiol, M., Formenton, G., Gilio, A.D., de Gennaro, G., Agostinelli, C., Pavoni, B. (2016). Carbonaceous $PM_{2.5}$ and secondary organic aerosol across the Veneto region (Ne Italy). Sci. Total Environ. 542, 172–181. https://doi.org/10.1016/j.scitotenv.2015.10.103

Lee, J.Y., Kim, Y.P., Kang, C.H., Ghim, Y.S. (2006). Seasonal trend of particulate PAHs at Gosan, a background site in Korea between 2001 and 2002 and major factors affecting their levels. Atmos. Res. 82, 680–687. https://doi.org/10.1016/j.atmosres.2006.02.022

Lewandowska, A., Staniszewska, M., Witkowska, A., Machuta, M., Falkowska, L. (2018). Benzo(a)pyrene parallel measurements in PM_1 and $PM_{2.5}$ in the coastal zone of the Gulf of Gdansk (Baltic Sea) in the heating and non-heating seasons. Environ. Sci. Pollut. Res. 25, 19458–19469. https://doi.org/10.1007/s11356-018-2089-9

Li, H., Wang, Y., Li, H., Zhu, C., Mao, H., Yang, M., Wang, R., Wang, W. (2016). Investigation of sources of atmospheric polycyclic aromatic hydrocarbons at Mount Lushan in southern China. J. Geophys. Res. 121, 3050–3061. https://doi.org/10.1002/2015JD024119

Li, X., Kong, S., Yin, Y., Li, L., Yuan, L., Li, Q., Xiao, H., Chen, K. (2016). Polycyclic aromatic hydrocarbons (PAHs) in atmospheric $PM_{2.5}$ around 2013 Asian Youth Games period in Nanjing. Atmos. Res. 174, 85–96. https://doi.org/10.1016/j.atmosres.2016.01.010

Lipiatou, E., Tolosa, I., Simo, R., Bouloubassi, I., Dachs, J., Marti, S., Sicre, M.A., Bayona, J.M., Grimalt, J.O., Saliot, A., Albaiges, J. (1997). Mass budget and dynamics of polycyclic aromatic hydrocarbons in the Mediterranean Sea. Deep Sea Res. Part II 44, 881–905. https://doi.org/10.1016/S0967-0645(96)00093-8

Liu, W., Wang, Y., Chen, Y., Tao, S., Liu, W. (2017). Polycyclic aromatic hydrocarbons in ambient air, surface soil and wheat grain near a large steel-smelting manufacturer in northern China. J. Environ. Sci. 57, 93–103. https://doi.org/10.1016/j.jes.2016.10.016

Ma, W.L., Liu, L.Y., Jia, H.L., Yang, M., Li, Y.F. (2018). PAHs in Chinese atmosphere Part I: Concentration, source and temperature dependence. Atmos. Environ. 173, 330-337. https://doi.org/10.1016/j.atmosenv.2017.11.029

Ma, X., Jia, H. (2016). Particulate matter and gaseous pollutions in three megacities over China: Situation and implication. Atmos. Environ. 140, 476–494. https://doi.org/10.1016/j.atmosenv.2016.06.008

Martiellini, T., Giannoni, M., Lepri, L., Katsoyiannis, A., Cincinelli, A. (2012). One year intensive $PM_{2.5}$ bound polycyclic aromatic hydrocarbons monitoring in the area of Tuscany, Italy. Concentrations, source understanding and implications. Environ. Pollut. 164, 252–258. https://doi.org/10.1016/j.envpol.2011.12.040

Meijer, S.N., Sweetman, A.J., Halsall, C.J., Jones, K.C. (2008). Temporal Trends of Polycyclic Aromatic Hydrocarbons in the U.K. Atmosphere: 1991-2005. Environ. Sci. Technol. 42, 3213–3218. https://doi.org/10.1021/es702979d

Mishra, N., Ayoko, G.A., Morawska, L. (2016). Atmospheric polycyclic aromatic hydrocarbons in the urban environment: Occurrence, toxicity and source apportionment. Environ. Pollut. 208, 110–117. https://doi.org/10.1016/j.envpol.2015.08.015

Moroni, B., Castellini, S., Crocchianti, S., Piazzalunga, A., Fermo, P., Scardazza, F., Cappelletti, D. (2015). Ground-based measurements of long-range transported aerosol at the rural regional background site of Monte Martano (Central Italy). Atmos. Res. 155, 26–36. https://doi.org/10.1016/j.atmosres.2014.11.021

Nguyen, T.N.T., Jung, K.S, Son, J.M., Kwon, H.O., Choi, S.D. (2018). Seasonal variation, phase distribution, and source identification of atmospheric polycyclic aromatic hydrocarbons at a semi-rural site in Ulsan, South Korea. Environ. Pollut. 236, 529–539. https://doi.org/10.1016/j.envpol.2018.01.080

Niu, X., Hang Ho, S.S., Ho, K.F., Huang, Y., Sun, J., Wang, Q., Zhou, Y., Zhao, Z., Cao, J. (2017). Atmospheric levels and cytotoxicity of polycyclic aromatic hydrocarbons and oxygenated-PAHs in $PM_{2.5}$ in the Beijing-Tianjin-Hebei region. Environ. Pollut. 231, 1075–1084. https://doi.org/10.1016/j.envpol.2017.08.099

Park, S.S., Kim, Y.J., Kang, C.H. (2002). Atmospheric polycyclic aromatic hydrocarbons in Seoul,

Korea. Atmos. Environ. 36, 2917–2924. https://doi.org/10.1016/S1352-2310(02)00206-6

Pekey, B., Karakas, D., Ayberk, S. (2007). Atmospheric deposition of polycyclic aromatic hydrocarbons to Izmit Bay, Turkey. Chemosphere 67, 537–547. https://doi.org/10.1016/j.chemosphere.2006.09.054

Pereira, G.M., Teinilä, K., Custódio, D., Gomes Santos, A., Xian, H., Hillamo, R., Alves, C.A., Bittencourt de Andrade, J., Olímpio da Rocha, G., Kumar, P., Balasubramanian, R., Andrade, M.D.F., de Castro Vasconcellos, P. (2017). Particulate pollutants in the Brazilian city of São Paulo: 1-year investigation for the chemical composition and source apportionment. Atmos. Chem. Phys. 17, 11943–11969. https://doi.org/10.5194/acp-17-11943-2017

Permadi, D.A., Kim Oanh, N.T., Vautard, R. (2018). Integrated emission inventory and modeling to assess distribution of particulate matter mass and black carbon composition in Southeast Asia. Atmos. Chem. Phys. 18, 2725–2747. https://doi.org/10.5194/acp-18-2725-2018

Pietrogrande, M.C., Abbaszade, G., Schnelle-Kreis, J., Bacco, D., Mecuriali, M., Zimmermann, R. (2011). Seasonal variation and source estimation of organic compounds in urban aerosol of Augsburg, Germany. Environ. Pollut. 159, 1861–1868. https://doi.org/10.1016/j.envpol.2011.03.023

Polachova, A., Gramblicka, T., Parizek, O., Sram, R.J., Stupak, M., Hajslova, J., Pulkrabova, J. (2020). Estimation of human exposure to polycyclic aromatic hydrocarbons (PAHs) based on the dietary and outdoor atmospheric monitoring in the Czech Republic. Environ. Res. 182, 108977. https://doi.org/10.1016/j.envres.2019.108977

Poor, N., Tremblay, R., Kay, H., Bhethanabotla, V., Swartz, E., Luther, M., Campbell, S. (2004). Atmospheric concentrations and dry deposition rates of polycyclic aromatic hydrocarbons (PAHs) for Tampa Bay, Florida, USA. Atmos. Environ. 38, 6005–6015. https://doi.org/10.1016/j.atmosenv.2004.06.037

Ravindra, K., Sokhia, R., Van Grieken, R. (2008). Atmospheric polycyclic aromatic hydrocarbons: Source attribution, emission factors and regulation. Atmos. Environ. 42, 2895–2921. https://doi.org/10.1016/j.atmosenv.2007.12.010

Ray, D., Chatterjee, A., Majumdar, D., Ghosh, S.K., Raha, S. (2017). Polycyclic aromatic hydrocarbons over a tropical urban and a high altitude Himalayan Station in India: Temporal variation and source apportionment. Atmos. Res. 197, 331–341. https://doi.org/10.1016/j.atmosres.2017.07.010

Rohde, H., Söderund, R., Ekstedt, J. (1980). Deposition of airborne pollution on the Baltic. Ambio 9, 168–173. https://www.jstor.org/stable/4312564

Roukos, J., Riffault, V., Locoge, N., Plaisance, H. (2009). VOC in an urban and industrial harbor on the French North Sea coast during two contrasted meteorological situations. Environ. Pollut. 157, 3001–3009. https://doi.org/10.1016/j.envpol.2009.05.059

Shahpoury, P., Lammel, G., Holubová Šmejkalová, A., Klánová, J., Přibylová, P., Váňa, M. (2015). Polycyclic aromatic hydrocarbons, polychlorinated biphenyls, and chlorinated pesticides in background air in central Europe – investigating parameters affecting wet scavenging of polycyclic aromatic hydrocarbons. Atmos. Chem. Phys. 15, 1795–1805. https://doi.org/10.5194/acp-15-1795-2015

Shi, G.L., Zhou, X.Y., Jiang, S.Y., Tian, Y.Z., Liu, G.R., Feng, Y.C., Chen, G., Liang, Y.K.X. (2015). Further insights into the composition, source, and toxicity of PAHs in size-resolved particulate matter in a megacity in China. Environ. Chemistry 3, 480–487. https://doi.org/10.1002/etc.2809

Šišović, A., Pehnec, G., Jakovljević, I., Šilović Hujić, M., Vadić, V., Bešlić, I. (2012). Polycyclic Aromatic Hydrocarbons at Different Crossroads in Zagreb, Croatia. Bull. Environ. Contam. Toxicol. 88, 438–442. https://doi.org/10.1007/s00128-011-0516-4

Siudek, P. (2018). Total carbon and benzo(a)pyrene in particulate matter over a Polish urban site – A combined effect of major anthropogenic sources and air mass transport. Atmos. Pollut. Res. 9, 764–773. https://doi.org/10.1016/j.apr.2018.01.001

Siudek, P., Frankowski, M. (2018a). The role of sources and atmospheric conditions in the seasonal variability of particulate phase PAHs at the urban site in central Poland. Aerosol Air Qual. Res. 18, 1405–1418. https://doi.org/10.4209/aaqr.2018.01.0037

Siudek, P. (2021). Inter-annual variability of trace elements in PM_{10} and the associated health risk in coastal-urban region (southern Baltic Sea, Poland). Urban Clim. 37, 100826. https://doi.org/10.1016/j.uclim.2021.100826

Slezakova, K., Reis, M.A., Pereira, M.C., Alvim-Ferraz, M.C. (2007). Influence of traffic on the elemental composition of PM_{10} and $PM_{2.5}$ in Oporto region. WIT Trans. Ecol. Environ. 101, 1743–3541. https://doi.org/10.2495/AIR070061

Staniszewska, M., Graca, B., Bełdowska, M., Saniewska, D. (2013). Factors controlling benzo(a)pyrene concentrations in aerosols in the urbanized coastal zone. A case study: Gdynia, Poland (Southern Baltic Sea). Environ. Sci. Pollut. Res. 20, 4154–4163. https://doi.org/10.1007/s11356-012-1315-0

Stohl, A., Wotawa, G., Seibert, P., Krompkolb H. (1995). Interpolation errors in wind fields as a function of spatial and temporal resolution and their impact on different types of kinematic trajectories. J. Appl. Meteorol. 34, 2149–2165. https://doi.org/10.1175/1520-0450(1995)034<2149:IEIWFA>2.0.CO;2

Stohl, A., Seibert, P. (1998). Accuracy of trajectories as determined from the conservation of meteorological tracers. Q. J. R. Meteorolog. Soc. 124, 1465–1484. https://doi.org/10.1002/qj.49712454907

Szabó, J., Szabó Nagy, A., Erdős, J. (2015). Ambient concentrations of PM_{10}, PM_{10}-bound polycyclic aromatic hydrocarbons and heavy metals in an urban site in Győr, Hungary. Air Qual. Atmos Health 8, 229–241. https://doi.org/10.1007/s11869-015-0318-7

Tsapakis, M., Apostolaki, M., Eisenreich, S., Stephanou, E.G. (2006). Atmospheric deposition and marine sediment fluxes of polycyclic aromatic hydrocarbons in the east Mediterranean Basin. Environ. Sci. Technol. 40, 4922–4927. https://doi.org/10.1021/es060487x

Upadhyay, N., Clements, A., Fraser, M., Herckes, P. (2011). Chemical speciation of $PM_{2.5}$ and PM_{10} in South Phoenix, AZ. J. Air Waste Manage. Assoc. 61, 302–310. https://doi.org/10.3155/1047-3289.61.3.302

Urbančok, D., Payne, A.J.R., Webster, R.D. (2017). Regional transport, source apportionment and health impact of PM_{10} bound polycyclic aromatic hydrocarbons in Singapore's atmosphere. Environ. Pollut. 229, 984–993. https://doi.org/10.1016/j.envpol.2017.07.086

Voivodeship raport (2020). Roczna ocena jakości powietrza w województwie pomorskim, raport wojewódzki za 2019 rok. Gdańsk, 1–106 (in Polish).

Wang, J., Cao, J., Dong, Z., Guinot, B., Gao, M., Huang, R., Han, Y., Huang, Y., Ho, S.S.H., Shen, Z. (2017). Seasonal variation, spatial distribution and source apportionment for polycyclic aromatic hydrocarbons (PAHs) at nineteen communities in Xi'an, China: The effects pf suburban scattered emissions in winter. Environ. Pollut. 231, 1330–1343. https://doi.org/10.1016/j.envpol.2017.08.106

Wang, Q., Liu, M., Yu, Y., Li, Y. (2016). Characterization and source apportionment of $PM_{2.5}$-bound polycyclic aromatic hydrocarbons from Shanghai city, China. Environ. Pollut. 218, 118–128. https://doi.org/10.1016/j.envpol.2016.08.037

Wiśniewska, K., Lewandowska, A.U., Staniszewska, M. (2019). Air quality at two stations (Gdynia and Rumia) located in the region of Gulf of Gdansk during periods of intensive smog in Poland. Air Qual. Atmos. and Health 12, 879–890. https://doi.org/10.1007/s11869-019-00708-6

Xu, G., Jiao, L., Zhang, B., Zhao, S., Yuan, M., Gu, Y., Liu, J., Tang, X. (2017). Spatial and Temporal Variability of the $PM_{2.5}/PM_{10}$ Ratio in Wuhan, Central China. Aerosol Air Qual. Res. 17, 741–751. https://doi.org/10.4209/aaqr.2016.09.0406

Yu, Q., Yang, W., Zhu, M., Gao, B., Li, S., Li, G., Fang, H., Zhou, H., Zhang, H., Wu, Z., Song, W., Tan, J., Zhang, Y., Bi, X., Chen, L., Wang, X. (2018). Ambient $PM_{2.5}$-bound polycyclic aromatic hydrocarbons (PAHs) in rural Beijing: Unabated with enhanced temporary emission control during the 2014 APEC summit and largely aggravated after the start of wintertime heating. Environ. Pollut. 238, 532–542. https://doi.org/10.1016/j.envpol.2018.03.079

Zhang, L., Cheng, I., Wu, Z., Harner, T., Schuster, J., Charland, J.P., Muir, D., Parnis, J.M. (2015). Dry deposition of polycyclic aromatic compounds to various land covers in the Athabasca oil sands region. J. Adv. Model. Earth Syst. 7, 1339–1350. https://doi.org/10.1002/2015MS000473

Zhang, Y., Tao, S. (2009). Global atmospheric emission inventory of polycyclic aromatic hydrocarbons (PAHs) for 2004. Atmos. Environ. 43, 812–819. https://doi.org/10.1016/j.atmosenv.2008.10.050